Solid–solid and solid–liquid equilibria in the *n*-alkanols family: C$_{18}$H$_{37}$OH–C$_{20}$H$_{41}$OH system

L. Ventolà,*^{a} T. Calvet,^{a} M. A. Cuevas-Diarte,^{a} H. A. J. Oonk^b and D. Mondieig^c

^{a} *Departament de Cristallografia, Mineralogia i Dipòsits Minerals, Facultat de Geologia, Universitat de Barcelona, Martí i Franquès s/n, E-08028, Barcelona, Spain. E-mail: lourdes_ventola@yahoo.com; Fax: +34 934021340; Tel: +34 934021350*
^{b} *Chemical Thermodynamics Group, Faculty of Chemistry, Debye Institute, Utrecht University, Padualaan 8, CH-3584, Utrecht, The Netherlands*
^{c} *Centre de Physique Moléculaire Optique et Hertzienne, UMR 5798 au CNRS Université Bordeaux I, Cours de la Libération 351, F-33405, Talence Cedex, France*

C$_{18}$H$_{37}$OH–C$_{20}$H$_{41}$OH is an example of a binary system showing isopolymorphism. The two alkanols display the same polymorphic behaviour. At low temperatures, they crystallize into the same ordered form γ (*C2/c*, *Z* = 8). On heating, γ transforms into the rotationally disordered form R$'_{IV}$ (*C2/m*, *Z* = 4), at a few degrees below the melting point of the latter. However, in most mixed samples of this system a β form (*P2$_1$/c*, *Z* = 8), metastable in the two pure components, has also been observed at low temperatures. At high temperatures, the β form transforms into the R$'_{II}$ form (*R$\bar{3}$m*, *Z* = 3). This R$'_{II}$ form is also metastable in the two pure components. The β form presents conformational defects, and molecules with all-*trans* conformation co-exist with molecules with CO-gt-conformation, in contrast, all the molecules in the γ form present all-*trans* conformation. In the R$'_{IV}$ form the rotational disorder is more accentuated than in the R$'_{IV}$ form. The disorder of composition (molecular alloys) stabilizes over wide ranges of compositions the β (disorder of conformation) and R$'_{II}$ (disorder of rotation) forms. Five solid–solid domains ([$\gamma + \beta$], [$\beta + R'_{II}$], [$\gamma + R'_{II}$], [$\gamma + R'_{IV}$] and [R$'_{II} + R'_{IV}$]) related by two peritectoid and eutectoid invariants, and two solid–liquid domains ([R$'_{IV} + $L] and [R$'_{II} + $L]) related by a eutectic and a peritectic invariant, are present. The [$\beta + R'_{II}$] domain has a minimum. All these domains are observed for compositions rich in the two pure components. The experimental phase diagram data are fully supported by the thermodynamically calculated phase diagram. The R$'_{II}$ + liquid domain has a width of less than 1 K; therefore, and due to the large heat effect, the system's alloys are good candidates for the storage of thermal energy.

Introduction

This research forms part of a general study of solid state miscibility in the *n*-alkanols family, and was carried out by the REALM† group (*Réseau Européen sur les Alliages Moléculaires*). We are interested in the preparation of molecular mixed crystals, the study of their crystallographic and thermodynamic properties and stability, the determination of their phase change behaviour, and their practical applications.[1–6] Therefore, our research is invariably focused on the study of different families of molecular substances: naphthalene derivatives, benzene derivatives, *n*-alkanes and *n*-alkanols.

The *n*-alkanols CH$_3$(CH$_2$)$_{n-1}$OH (abbreviated here as C$_n$H$_{2n+1}$OH) are among the simplest of the substituted hydrocarbons. A single –OH group replaces a hydrogen atom at one end of the aliphatic chain, forming hydrogen bonds between the chains. From an applications point of view, the *n*-alkanols and their alloys are promising candidates for storing thermal energy due to their high fusion heat.

In terms of fundamentals, the study of this family of substances offers the opportunity to define behavioural rules inside the family and correlate their properties with those of other families, with different types of configurations and interactions, studied by the REALM group.

† The REALM is integrated by four European Universities: Universitat de Barcelona, Universitat Politècnica de Catalunya, Utrecht University and Université Bordeaux I.

In this paper we report a detailed study of a binary system between two *n*-alkanols, C$_{18}$H$_{37}$OH and C$_{20}$H$_{41}$OH. The study of this system is of interest for a number of reasons. Firstly, to our knowledge no such study has yet been published. Secondly, the REALM experience of the *n*-alkanes family,[7,8] is that in systems like this, where two pure compounds have the same polymorphic behaviour, the phase diagram can not always be interpreted in terms of simple isomorphism or simple isodimorphism. Indeed, it is often necessary to use crossed[9,10] or double crossed[10,11] isodimorphism terms in order to explain the phase diagram. Finally, the study of this and other systems in the *n*-alkanols family[12] will allow us to define behavioural rules that will explain the effects of substitution, orientation and conformation disorder.

In previous studies of binary alkanol systems,[13] it was observed that the behaviour of mixed samples depends on the method of sample preparation: dissolution–evaporation (D + E) or melting–quenching (M + Q). Therefore, in order to avoid metastability, solid–solid transitions were only studied using samples prepared by D + E. The solid to liquid transitions were studied using samples prepared by both methods (on D + E and M + Q).

Experimental

The C$_{18}$H$_{37}$OH and C$_{20}$H$_{41}$OH were purchased from Fluka Chemical, labelled ≥98% pure, and were used without further

purifications. The purity of these substances was corroborated by gas chromatography (CG).

The mixed samples were obtained by either dissolution–evaporation (D + E), or melting–quenching (M + Q) methods. In the D + E method the components are weighed in the desired proportions and dissolved with diethyl ether; the solvent is then quickly evaporated. In the M + Q method the components are weighed in the desired proportions, melted and mixed to give a homogeneous sample and then quenched into liquid nitrogen.

The samples were characterised by differential scanning calorimetry (DSC) and X-ray powder diffraction (XRD). Calorimetric measurements were taken with a Perkin–Elmer DSC-7 calorimeter. The following conditions were adopted during the analysis:

- Sample weight: between 3.9 and 4.1 mg
- Scanning rate: 2 K min^{-1}
- Six independent measurements for each sample

The instrument was calibrated with the use of the known melting temperature and enthalpy indium standard, as well as the melting temperature of the *n*-decane standard.

The random part of the uncertainties was estimated using the Student's method with a 95% threshold of reliability.

From the DSC curves the characteristic temperatures were determined by the shape factor method.[14] Enthalpy effects were evaluated by integration of the DSC signals.

X-Ray powder diffraction measurements were taken using a Siemens D-500 diffractometer and a Guinier–Simon camera. The Siemens D-500 diffractometer uses Bragg–Brentano geometry, Cu-Kα radiation and a secondary monochromator. The data were collected at different temperatures using an Anton PAAR TTK system with a heating rate of 0.02 K s^{-1} and 5 min of stabilisation time. The analysis performed consists of a heating process from 298 K up to the melting temperature. The patterns were scanned with a step size of 0.025° and step time of 5 s; the 2θ range was 1.6–60°. The cell parameters were refined using the "Pattern-Matching" option of the FULLPROF[15] program.

The Guinier–Simon cameraworks in transmission mode using Cu-Kα radiation, with a quartz crystal as the primary monochromator. The sample was mounted on a rotating sealed capillary of 0.5 mm diameter, perpendicular to the X-ray radiation beam and the window width used was 1.5 mm. The sample was heated at 0.5 K min^{-1}. The continuous evolution of the X-ray pattern is registered on a photographic film, which is moved perpendicularly to the beam at a constant rate of 1 mm h^{-1}.

The pure *n*-alkanols

The pure *n*-alkanols, $C_{18}H_{37}OH$ and $C_{20}H_{41}OH$, crystallize into the same pair of solid forms. The γ form,[16–19] which is stable at low temperatures, is an ordered form with a monoclinic symmetry (space group $C2/c$, $Z = 8$) in which all C–C bonds of the molecules have the *trans* conformation. In this study we applied the non-conventional space group, $A2/a$, to facilitate the comparison between the different forms. In a previous work[16] we showed how a metastable form appears when these alkanols are subjected to a melting–quenching process. This metastable form is isostructural to the β form[20] ($P2_1/c$, $Z = 8$) observed in the alkanols with an odd number of carbons. The β form contains two molecules in the asymmetric unit, each one being a different rotational isomer and disposed alternatively: the first isomer is an all-*trans* conformer (similar to the γ form) while the second has all the C–C–C–C torsion angles in *trans* form and the C–C–C–O torsion angle in *gauche* form. A few degrees below the melting point the γ form changes into the rotationally disordered form R'_{IV} ($C2/m$, $Z = 4$).[16,18] In addition to the orientational disorder of the full chains, there are what are known as *gauche* defects at the end

of the chains. The thermodynamic and structural characteristics of the two alkanols used in the present research are detailed in Tables 1 and 2.

Phase diagram

In order to determine the phase diagram (Fig. 1) nineteen mixed compositions of the system were studied.

A crystallographic analysis under isoplethic conditions revealed that molecular alloys having the symmetry of the pure components are only found for compositions of more than 98% in $C_{18}H_{37}OH$ and more than 95% in $C_{20}H_{41}OH$. For the remaining intermediate compositions forms are found that are absent (as a stable form) for the components: these are the forms β ($P2_1/c$, $Z = 8$) and R'_{II} ($R\bar{3}m$, $Z = 3$). At 293 K the β form was observed between 5 and 70 mol% in $C_{20}H_{41}OH$. The R'_{II} form melts in most compositions: between $5 < x < 80$ mol% in $C_{20}H_{41}OH$. In the phase diagram the existence of these metastable forms in the pure components is linked to the existence of five solid–solid domains ([$\gamma + \beta$], [$\beta + R'_{II}$], [$\gamma + R'_{II}$], [$\gamma + R'_{IV}$] and [$R'_{II} + R'_{IV}$]), and two solid–liquid domains ([$R'_{IV} + L$] and [$R'_{II} + L$]). All these domains were observed not only for the compositions rich in $C_{18}H_{37}OH$ but also for those in $C_{20}H_{41}OH$, where the majority of these domains are larger than in the former. At 293 K the [$\gamma + \beta$] domains were observed between 2 and 5 mol% in $C_{20}H_{41}OH$, and between 70 and 95 mol% in $C_{20}H_{41}OH$. These limits were determined from the reticular distance d_{006} evolution *vs.* the composition for the two phases involved (Fig. 2). On heating, these [$\gamma + \beta$] domains are related by a peritectoid invariant with two other solid–solid domains ([$\gamma + R'_{II}$] and [$\beta + R'_{II}$]). For the compositions rich in $C_{18}H_{37}OH$ this invariant is placed at $\approx$321.0 K between 2 and 15 mol% in $C_{20}H_{41}OH$, and for the compositions rich in $C_{20}H_{41}OH$ it is placed at $\approx$321.5 K, in this case between 60 and 90 mol% in $C_{20}H_{41}OH$.

By increasing the temperature, we observed how the [$\gamma + R'_{II}$] domain is linked by a eutectoid invariant to two other solid–solid domains ([$\gamma + R'_{IV}$] and [$R'_{II} + R'_{IV}$]). In this case, the invariants are situated at $\approx$325.8 K between 2 and 7 mol% in $C_{20}H_{41}OH$, and at $\approx$331.3 K between 80 and 95 mol% in $C_{20}H_{41}OH$.

Finally, at higher temperatures we observed how the [$R'_{II} + R'_{IV}$] domain is linked to [$R'_{II} + L$] and [$R'_{IV} + L$] domains by an eutectic invariant at 329.5 K between 3 and 5 mol% in $C_{20}H_{41}OH$, and by a peritectic invariant at $\approx$334.2 K between 80 and 90 mol% in $C_{20}H_{41}OH$. The width of these [solid + liquid] domains is not larger than 1 K.

Table 1 Temperatures (T/K) and enthalpy (ΔH/kJ mol^{-1}) transitions for $C_{18}H_{37}OH$ and $C_{20}H_{41}OH$

	$T_{transition}$	$\Delta H_{transition}$	$T_{melting}$	$\Delta H_{melting}$	Ref.
$C_{18}H_{37}OH$	329.5 ± 0.5	26.5 ± 1.8	330.3 ± 0.5	40.1 ± 1.0	16
$C_{20}H_{41}OH$	335.5 ± 0.5	28.4 ± 0.4	336.6 ± 0.5	43.6 ± 1.3	16

Table 2 Cell parameters of the γ ($A2/a$, $Z = 8$) and R'_{IV} ($C2/c$, $Z = 4$) forms at 293 K for $C_{18}H_{37}OH$ and $C_{20}H_{41}OH$

	a/Å	b/Å	c/Å	β/°	Phase	Ref.
$C_{18}H_{37}OH$	9.031(3)	4.959(3)	98.15(5)	122.41(5)	γ	16
	8.458(3)	4.933(4)	48.58(6)	92.1(1)	R'_{IV}	16
$C_{20}H_{41}OH$	9.035(3)	4.970(4)	108.71(9)	122.84(4)	γ	17
	8.450(5)	4.940(7)	53.24(8)	93.7(2)	R'_{IV}	16
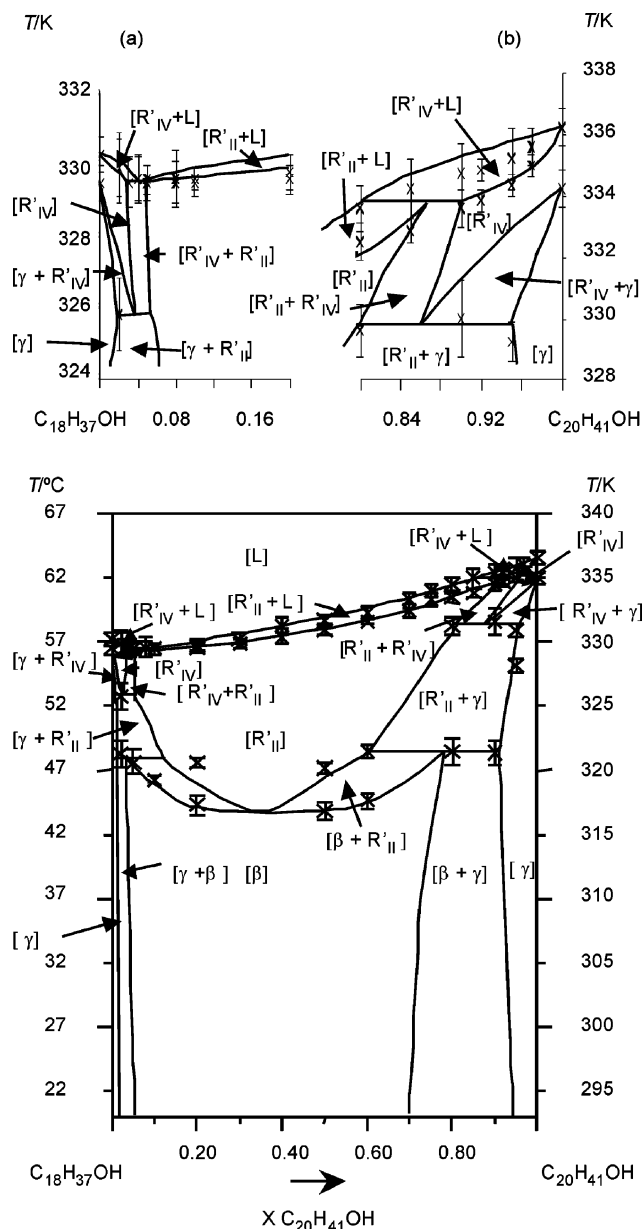
Fig. 1 Experimental phase diagram of the $C_{18}H_{37}OH$–$C_{20}H_{41}OH$ system. (a) Zoom at high temperature for the compositions rich in $C_{18}H_{37}OH$. (b) Zoom at high temperature for the compositions rich in $C_{20}H_{41}OH$.
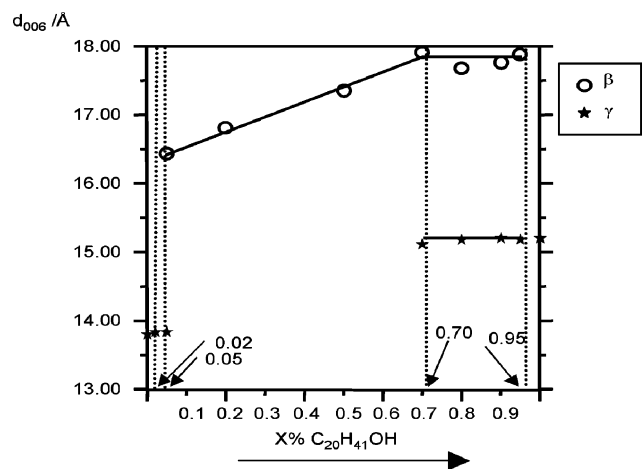
Fig. 2 Variations of d_{006} vs. composition of the γ and β forms at 293 K.
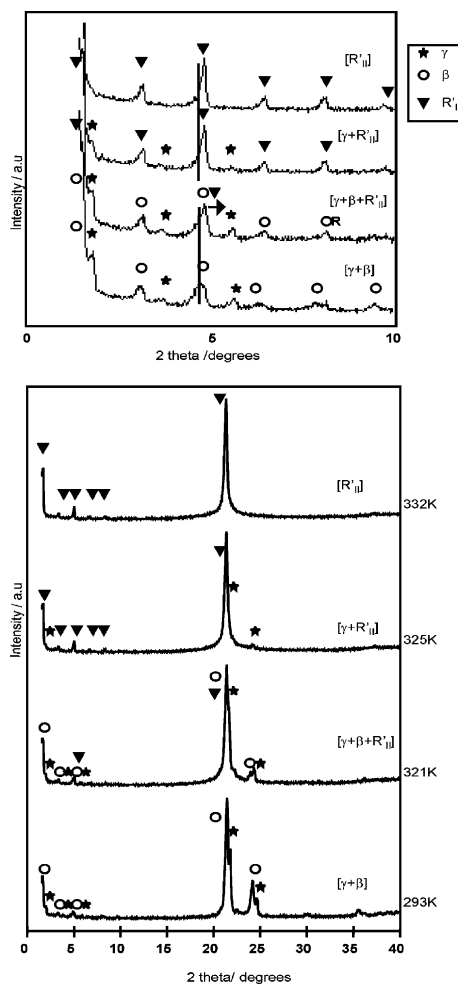
Fig. 3 X-Ray diffraction diagrams at the temperature where γ and β phases coexist, and at the temperatures where R'_{II} appears. When phase R'_{II} appears, the spectrum background rises and the 00*l* reflections shift slightly to higher 2θ angles with respect to β phase reflections. The upper part of the figure exhibits the enlarged low 2θ angles.

Table 3 Cell parameters of the β ($P2_1/c$, $Z = 8$) and γ ($A2/a$, $Z = 8$) forms at 293 K for the mixed compositions

x $C_{20}H_{41}OH$	$a/\text{Å}$	$b/\text{Å}$	$c/\text{Å}$	$\beta/°$	Phase
0.02	9.019(8)	4.958(4)	98.1(1)	122.35(7)	γ
0.05	5.030(1)	7.410(1)	99.4(1)	90.70(1)	β
0.20	5.028(3)	7.408(3)	101.3(2)	90.90(2)	β
0.50	5.029(4)	7.410(4)	105.2(1)	90.90(7)	β
0.70	9.03(1)	4.94(1)	107.9(1)	122.6(1)	γ
0.80	9.03(2)	4.95(1)	108.3(2)	122.1(1)	γ
	5.02(1)	7.40(2)	105.8(1)	91.00(2)	β
0.90	9.02(1)	4.96(1)	108.3(1)	122.7(1)	γ
0.95	9.01(2)	4.95(1)	108.2(1)	122.6(1)	γ

Table 4 Cell parameters of the R'_{II} (R $\bar{3}m$, $Z = 3$) form at 329 K for the mixed compositions

x $C_{20}H_{41}OH$	$a/\text{Å}$	$b/\text{Å}$	$c/\text{Å}$	$\gamma/°$
0.10	4.823(6)	4.823(6)	148.3(6)	120
0.20	4.829(9)	4.829(9)	151.6(6)	120
0.50	4.825(6)	4.825(6)	155.6(6)	120
0.60	4.808(6)	4.808(6)	156.8(9)	120
0.70	4.802(6)	4.802(6)	160.2(6)	120

Table 5 Temperatures (T/K) and enthalpy (ΔH/kJ mol^{-1}) transitions for the mixed compositions. T_E and T_P are eutectic and peritectic invariants, respectively. Subscript 1 is used to refer to compositions rich in C$_{18}$H$_{37}$OH and subscript 2 is used for compositions rich in C$_{20}$H$_{41}$OH

	T	ΔH	T_{solvi}	T_{solvf}	T_{P1}	T_{P2}	T_{E1}	T_{E2}	T_E	T_P	T_{sol}	T_{liq}	$T_{melting}$	$\Delta H_{melting}$
	$\gamma \to$ R$'_{IV}$										**R$'_{IV} \to$ L**			
C$_{18}$H$_{37}$OH	329.5 ± 0.5	26.5 ± 2.3											330.3 ± 0.5	40.1 ± 1.8
0.02					321.3 ± 1.0		325.8 ± 1.0				329.9 ± 0.8	329.9 ± 1.0		
0.03									329.5 ± 0.7			329.5 ± 0.7		
0.04									329.6 ± 0.6			329.6 ± 0.7		
0.05					320.7 ± 0.9				329.5 ± 0.5			329.6 ± 0.4		
			$\beta \to$ R$'_{II}$								**R$'_{II} \to$ L**			
0.08											329.5 ± 0.6	329.6 ± 0.8		
0.10			319.3 ± 0.3								329.5 ± 0.4	329.6 ± 0.3		39.4 ± 1.0
0.20			317.3 ± 0.8	320.6 ± 0.3							329.6 ± 0.4	329.8 ± 0.5		39.8 ± 1.1
0.30											329.9 ± 0.3	330.3 ± 0.4		39.5 ± 1.3
0.40											330.5 ± 0.6	331.3 ± 0.6		40.2 ± 1.0
0.50			316.9 ± 0.7	320.2 ± 0.4							331.0 ± 0.4	331.7 ± 0.4		40.2 ± 1.0
0.60			317.7 ± 0.6	—		321.5 ± 0.5					331.7 ± 0.3	332.3 ± 0.5		40.7 ± 0.5
0.70											332.5 ± 0.5	333.3 ± 0.6		40.8 ± 1.0
0.75											333.3 ± 0.5	334.0 ± 0.5		
0.80						321.5 ± 1.0		331.3 ± 0.7			333.6 ± 0.5	334.5 ± 0.6		
											R$'_{IV} \to$ L			
0.85										333.9 ± 0.3		335.0 ± 0.8		
0.90						321.4 ± 1.0		331.6 ± 0.0		334.5 ± 0.5		335.4 ± 0.8		42.4 ± 1.0
			$\gamma \to$ R$'_{II}$											
0.92			328.2 ± 0.5	—							334.7 ± 0.3	335.5 ± 0.3		
0.95								331.0 ± 0.5			335.1 ± 0.3	335.8 ± 0.8		
0.97											335.6 ± 0.3	336.1 ± 0.5		

The temperatures of the three-phase equilibria were determined by DSC analysis, and confirmed by X-ray diffraction; the exception to this was the eutectoid invariant placed at 325.8 K, between 2 and 7% mol in $C_{20}H_{41}OH$, which was deduced from an overall phase diagram analysis. As an example, Fig. 3 shows the X-ray diffraction diagrams at different temperatures for the 80 mol% in the $C_{20}H_{41}OH$ composition. At the temperatures where the rotator phase appears, in this case R'_{II} at 321 K, there is a rise of background spectrum and a thin displacement of the 00l reflections to a high 2θ angle compared with the β phase. Furthermore, there is a decrease in the β reflections intensity with a rise in temperature, until this phase disappears at 325 K. All this indicates the presence of the R'_{II} form.

For some compositions, the cell parameters of the γ and β forms were determined at 293 K, and for the R'_{II} form at 329 K (Tables 3 and 4, respectively).

The temperature and energy transitions of the mixed samples were determined by DSC (Table 5).

At the end of this section, attention should be given to the difficulties we experienced with samples containing 20–50 mol% of $C_{20}H_{41}OH$. For reasons not yet understood, we did not succeed in obtaining clear DSC signals for the change from the 'ordered' form β to the rotator form R'_{II}. A fact is that an amount of solvent (diethyl ether) is remaining in the material; it can be smelled after a long period of time (two years), and, also, be indicated by gas chromatography. And, unlike the samples for the other compositions, which are powdery, samples between 20 and 50% have a sticky aspect. Attempts to remove the difficulties by using other solvents (such as acetone and dichloromethane) were unsuccessful.

Notwithstanding this inconvenience, the reliable part of the collection of experimental data clearly points at the presence of a minimum. By thermodynamic analysis, see hereafter, the minimum in the [$\beta + R'_{II}$] two-phase region was calculated at 35 mol% and $T = 316.5$ K.

Thermodynamic analysis

The thermodynamic analysis of the phase diagram (Fig. 4) has been carried out in terms of the EGC methodology,[21] applying the ideas of crossed isodimorphism and isopolymorphism. In this approach, two-phase regions are, first, analysed in an individual manner (LIQFIT[22]), and, subsequently, combined to the stable phase diagram (by means of PROPHASE[23]). In the individual analyses the two-phase regions are optimized; and therewith the difference in excess Gibbs energy, ΔG^E, between the two phases. As in the case of the $C_{19}H_{39}OH$–$C_{20}H_{41}OH$ system,[12] we applied two simplifications: Gibbs energies ($G = H - TS$) were taken as linear functions of temperature (where by enthalpy, H, and entropy, S, become independent of temperature); and liquid mixtures were taken as ideal mixtures (negligence of excess properties).
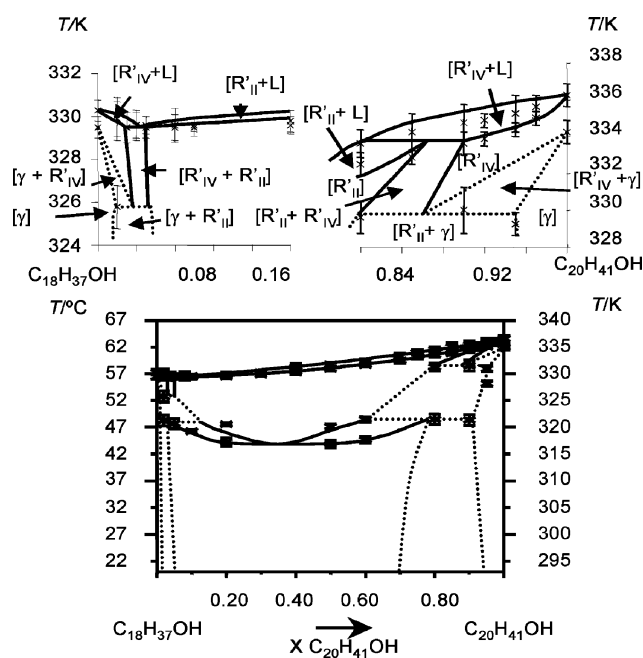
Solid–liquid equilibria: for the $R'_{IV} + L$ equilibrium modelling we used the melting properties of the pure components and the experimental liquidus. However, for the $R'_{II} + L$ equilibrium modelling, the transition properties of the metastable forms of the pure components were used. The metastable temperatures were obtained by interpolating a polynomial fit of the values of the n-alkanols where this form is stable, and with the values obtained by the extrapolation of the [$R'_{II} + L$] domain in other binary systems where this domain is observed in a wide range of compositions. In energy terms the R'_{II} and R'_{IV} forms are very similar. For the different n-alkanols studied, the $\Delta H_{R'_{II} \to L}$ and $\Delta H_{R'_{IV} \to L}$ vs. n data can be fitted with a single polynomial function (degree 2).[24] ΔS values were obtained by considering: $\Delta H^m_{R'_{II} \to L} = \Delta H^s_{R'_{IV} \to L}$ (m: metastable, s: stable). The values used were: $T^m_{R'_{II} \to L} = 329.8$ K, $\Delta S^m_{R'_{II} \to L} = 121.6$ J K mol^{-1} for $C_{18}H_{37}OH$ and $T^m_{R'_{II} \to L} = 335.7$ K, $\Delta S^m_{R'_{II} \to L} = 129.9$ J K mol^{-1} for $C_{20}H_{41}OH$. The $G^{E,R'_{IV}}$ and $G^{E,R'_{II}}$ values obtained are presented in Table 6.

Solid–solid equilibria: for the $\beta + R'_{II}$ equilibrium modelling, the $G^{E,R'_{II}}$ values and the metastable transition properties of the pure components were used to calculate $G^{E,\beta}$ (Table 6). The values of the transition properties used were $T^m_{\beta \to R'_{II}} = 323.9$ K, $\Delta S^m_{\beta \to R'_{II}} = 81.8$ J K mol^{-1} for $C_{18}H_{37}OH$, and $T^m_{\beta \to R'_{II}} = 328.3$ K, $\Delta S^m_{\beta \to R'_{II}} = 86.5$ J K mol^{-1} for $C_{20}H_{41}OH$. The temperatures were obtained by the [$\beta + R'_{II}$] domain extrapolation, and the ΔS values were calculated by considering $\Delta H^m_{\beta \to R'_{II}} = \Delta H^s_{\gamma \to R'_{II}}$. In this case, the adjustment was made with the superior solvus curve of the $\beta + R'_{II}$ equilibrium. It was not possible to model the other solid–solid equilibria, as insufficient experimental values were available.

Conclusions

The two alkanols $C_{18}H_{37}OH$ and $C_{20}H_{41}OH$ display the same polymorphic behaviour. The form stable at low temperature is the ordered form γ, where all C–C bonds in the polymethylene chain, and the C–O bond are in all-*trans* conformation. The γ form changes into the rotator form R'_{IV}, a few degrees below the melting point of the latter. The R'_{IV} form has rotational disorder in the carbon chain, and CO gt- (end-*gauche*) conformational defects.

In mixtures of the two alkanols, two additional forms, β and R'_{II}, make a stable appearance; and so over a wide range of compositions. It is observed that the substitutional disorder of the molecules in the crystal lattice has the effect of enlacing the other types of disorder: the presence of molecules with (CO gt-) end defects in the 'ordered' form β; highest degree of

Fig. 4 Calculated phase diagram. Continuous lines represent calculated results and dotted lines interpreted ones; $\times$ represent the experimental points. (a) Zoom at high temperature for the compositions rich in $C_{18}H_{37}OH$. (b) Zoom at high temperature for compositions rich in $C_{20}H_{41}OH$.

Table 6 Coefficients of the excess Gibbs energy ($G^E = x(1 - x)[G_1 + G_2(1 - 2x)]$) of the different solid forms (G^E in J mol^{-1})

	G^E_1	G^E_2
R'_{IV}	2087.4	578.2
R'_{II}	677.5	263.4
β	2627.5	1645.2

rotational disorder and end-*gauche* defects in R'_{II} (similar to R_{II} in *n*-alkane mixtures).

The rich polymorphic behaviour of the system corresponds to a complex *TX* phase diagram. The diagram is an example of isopolymorphism: limited miscibility in all of the four solid forms. The forms β and R'_{II} have wide simple-phase fields; the 'pure-component forms' γ and R'_{IV}, as a result, have narrow simple phase fields.

The experimental phase-diagram data are fully supported by the outcome of a thermodynamic analysis. One aspect of the diagram is the minimum, found by calculation, in the $[\beta + R'_{II}]$ two-phase region. The existence of the minimum could not be demonstrated by experimentation: for some reason, suitable samples could not be prepared for compositions around 35 mol% in $C_{20}H_{41}OH$.

The $[R'_{II} + L]$ solid–liquid two-phase region, extending over 80% of the composition range, has a thermal window of less than 1 K. Alloys of $C_{18}H_{37}OH$ and $C_{20}H_{41}OH$, because of that fact, are excellent phase change materials for applications – storage of energy; thermal protection – in the range of 57–61 °C.

Acknowledgements

References

1 M. A. Cuevas-Diarte, N. B. Chanh and Y. Haget, *Mater. Res. Bull.*, 1987, **22**, 985.
2 Y. Haget, *J. Chim. Phys.*, 1993, **90**, 313.
3 D. Mondieig, A. Marbeuf, L. Robles, P. Espeau, B. Porier, Y. Haget, T. Calvet-Pallas and M. A. Cuevas-Diarte, *High Temp. High Pressures*, 1997, **29**, 385.
4 H. A. J. Oonk, D. Mondieig, Y. Haget and M. A. Cuevas-Diarte, *J. Chem. Phys.*, 1998, **108**, 715.
5 Y. Haget, D. Mondieig and M. A. Cuevas-Diarte, *Fr. Pat.*, FR 91/08695, 1999; *Eur. Pat.*, EP 92915596.8, 1999 and *US Pat.*, US 07 988, 1999.
6 Y. Haget, D. Mondieig and M. A. Cuevas-Diarte, Depot de marque ALCAL®, Centre National de la Recherche Scientifique, France, 1993.
7 F. Rajabalee, V. Métivaud, D. Mondieig, Y. Haget and M. A. Cuevas-Diarte, *J. Mater. Res.*, 1999, **14**(6), 2644.
8 V. Métivaud, F. Rajabalee, D. Mondieig, Y. Haget and M. A. Cuevas-Diarte, *Chem. Mater.*, 1999, **11**(1), 117.
9 L. C. Pardo, M. Barrio, J. Ll. Tamarit, D. O. López, J. Salut, P. Négrier and D. Mondieig, *Phys. Chem. Chem. Phys.*, 2001, **3**, 2644.
10 M. A. Cuevas-Diarte, P. Espeau, Y. Haget, D. Mondieig, H. A. J. Oonk and L. Robles, *XXI Journées des Equilibres entre Phases*, Université Rouen, France, 1995, p. 63.
11 P. Espeau, European thesis, Université Bordeaux I, France, 1995.
12 L. Ventolà, T. Calvet, M. A. Cuevas-Diarte, D. Mondieig and H. A. J. Oonk, *Phys. Chem. Chem. Phys.*, 2002, **4**, 1953.
13 L. Ventolà, T. Calvet, M. A. Cuevas-Diarte, D. Mondieig and J. C. van Miltenburg, *Phys. Chem. Chem. Phys.*, 2003, **5**, 947.
14 R. Courchinoux, N. B. Chanh, Y. Haget, T. Calvet, E. Estop and M. A. Cuevas-Diarte, *J. Chim. Phys.*, 1989, **86**(3), 561.
15 J. Rodriguez-Carvajal, FULLPROF, a program for Rietveld refinement and pattern matching analyses; Abstracts of the satellite meeting on powder diffraction of the XVth congress of the International Union of Crystallography, Toulouse, 1990, p. 117.
16 L. Ventolà, M. Ramírez, T. Calvet, X. Solans, M. A. Cuevas-Diarte, N. Negrier, D. Mondieig, J. C. van Miltenburg and H. A. J. Oonk, *Chem. Mater.*, 2002, **14**, 508.
17 F. Michaud, L. Ventolà, T. Calvet, M. A. Cuevas-Diarte, X. Solans and M. Font-Bardia, *Acta Crystallogr., Sect. C*, 2000, **56**, 219.
18 T. Seto, *Mem. Collect. Sci. Univ. Kyoto*, 1962, **A89**, 30.
19 K. Fujimoto, T. Yamamoto and T. Hara, *Rep. Prog. Polym. Phys. Jpn.*, 1985, **28**, 163.
20 D. Precht, *Fette Seifen Anstrichm.*, 1976, **4**, 145.
21 J. A. Bouwstra, N. Brouwer, A. C. G. Van Genderen and H. A. J. Oonk, *Thermochim. Acta*, 1980, **38**, 97.
22 M. H. G. Jacobs and H. A. J. Oonk, LIQFIT program, Utrecht University, Netherlands, 1989.
23 J. S. van Duijneveldt, F. S. A. Baas and H. A. J. Oonk, PROPHASE program, Utrecht University, Netherlands, 1988.
24 L. Ventolà, T. Calvet, M. A. Cuevas-Diarte, M. Ramírez, H. A. J. Oonk and D. Mondieig, *Phys. Chem. Chem. Phys.*, 2004, **6**, 1786.